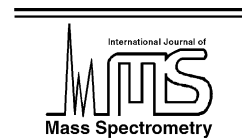




ELSEVIER

International Journal of Mass Spectrometry 227 (2003) 619–625



www.elsevier.com/locate/ijms

Subject index Volume 227

Ab initio calculations

Sequential bond energies of $\text{Pt}^+(\text{NH}_3)_x$ ($x = 1-4$) determined by collision-induced dissociation and theory, 47

The gas and solution phase acidities of HNO, HOONO, HONO, and HONO₂, 421

Tautomerization and dissociation of ethylene phosphonate ions $[\text{OCH}_2\text{CH}_2\text{O}]\text{P}(\text{H})\text{O}^+$: an experimental and CBS-QB3 computational study, 453

Aerosol

Abiotic synthesis of ATP from AMP in the gas phase: implications for the origin of biologically important molecules from small molecular clusters, 147

Ag_n^+

Dissociation energies of silver clusters Ag_n^+ , $n = 14, 15, 16, 18, 87$

Agnostic interactions

Binding energies of Cu^+ to saturated and α, β -unsaturated alkanes, silanes and germanes. The role of agnostic interactions, 401

Alkali metal

Alkali metal binding energies of dibenzo-18-crown-6: experimental and computational results, 63

Alkali metal ions

Cation- π interactions with a model for an extended π network. Absolute binding energies of alkali metal cation-naphthalene complexes determined by threshold collision-induced dissociation and theoretical studies, 1

Influence of substituents on cation- π interactions. 3. Absolute binding energies of alkali metal cation-aniline complexes determined by threshold collision-induced dissociation and theoretical studies, 339

Amino acids

Structures and fragmentations of zinc(II) complexes of amino acids in the gas phase. IV. Solvent effect on the structure of electro sprayed ions, 439

The Na^+ affinities of α -amino acids: side-chain substituent effects, 509

API/MS

The effect of liquid chromatography eluents and additives on the positive ion responses of cocaine, benzoylecgonine, and ecgonine methyl ester using electrospray ionization, 247

ATP

Abiotic synthesis of ATP from AMP in the gas phase: implications for the origin of biologically important molecules from small molecular clusters, 147

Basicity

The proton affinity scale, and effects of ion structure and solvation, 525

Proton affinities and gas-phase basicities: theoretical methods and structural effects, 601

Benzene

Kinetics and thermodynamics for the bonding of benzene to 20 main-group atomic cations: formation of half-sandwiches, full-sandwiches and beyond, 563

Benzoylecgonine

The effect of liquid chromatography eluents and additives on the positive ion responses of cocaine, benzoylecgonine, and ecgonine methyl ester using electrospray ionization, 247

Bidentate bases

Application of the kinetic method to bifunctional bases. MIKE and CID-MIKE test cases, 479

Blackbody-induced dissociation

Dissociation of *p*-cymene molecular ions induced by thermal radiation, 135

Bond dissociation energies

Cation- π interactions with a model for an extended π network. Absolute binding energies of alkali metal cation-naphthalene complexes determined by threshold collision-induced dissociation and theoretical studies, 1

Influence of substituents on cation- π interactions. 3. Absolute binding energies of alkali metal cation-aniline complexes determined by threshold collision-induced dissociation and theoretical studies, 339

Bond energies

Guided ion beam studies of transition metal-ligand thermochemistry, 289

Bond strength

G3 and G2 thermochemistry of sulfur fluoride neutrals and anions, 413

Branching ratios

Branching ratios for the dissociative recombination of hydrocarbon ions. I: The cases of C_4H_9^+ and C_4H_5^+ , 273

Calculation

Proton affinity of some radicals of alcohols, ethers and amines, 373

Gas phase basicity of silanaldehydes and silanones, 381

Capping agents

3-Dimensional structural characterization of cationized polyhedral oligomeric silsesquioxanes (POSS) with styryl and phenylethyl capping agents, 205

Catalysis

Tautomerization and dissociation of ethylene phosphonate ions $[\text{OCH}_2\text{CH}_2\text{O}]\text{P}(\text{H})\text{O}^+$: an experimental and CBS-QB3 computational study, 453

Cation- π interactions

Cation- π interactions with a model for an extended π network. Absolute binding energies of alkali metal cation-naphthalene complexes determined by threshold collision-induced dissociation and theoretical studies, 1

Influence of substituents on cation- π interactions. 3. Absolute binding energies of alkali metal cation-aniline complexes determined by threshold collision-induced dissociation and theoretical studies, 339

CBS-QB3

Tautomerization and dissociation of ethylene phosphonate ions $[-\text{OCH}_2\text{CH}_2\text{O}]\text{P}(\text{H})=\text{O}^+$: an experimental and CBS-QB3 computational study, 453

4-Center transition state

Stereochemical analysis of deuterated alkyl chains by charge-remote fragmentations of protonated parent ions, 175

Charge solvation

The Na^+ affinities of α -amino acids: side-chain substituent effects, 509

Chiroselective octamer of serine

An electrospray ionization-flow tube study of H/D exchange in the protonated serine dimer and protonated serine dipeptide, 77

Chloro-substitution effects

How does chlorine substitution on acetonitrile affect the internal $\text{S}_{\text{N}}2$ isomerization of proton-bound pairs $(\text{ClCH}_2\text{CN})(\text{ROH})\text{H}^+$ ($\text{R} = \text{CH}_3, \text{C}_2\text{H}_5, \text{C}_3\text{H}_7$)?, 471

CID

Gas-phase ion chemistry and ion thermochemistry of phenyltrifluorosilane, 303

New measurements of the thermochemistry of SF_5^- and SF_6^- , 361

Cluster ion

Thermochemical stabilities of the gas-phase cluster ions $\text{H}_3\text{C}^+(\text{N}_2)_n$, 391

How does chlorine substitution on acetonitrile affect the internal $\text{S}_{\text{N}}2$ isomerization of proton-bound pairs $(\text{ClCH}_2\text{CN})(\text{ROH})\text{H}^+$ ($\text{R} = \text{CH}_3, \text{C}_2\text{H}_5, \text{C}_3\text{H}_7$)?, 471

Clusters

Guided ion beam studies of transition metal-ligand thermochemistry, 289

Comparison of methyl and hydroxyl protons generated in a Coulomb explosion event: application of a time-of-flight gating technique to methanol clusters, 577

CO

Gas-phase kinetic measurements and quantum chemical calculations of the ligation of Ni^+ , Cu^+ , $\text{Ni}^+(\text{pyrrole})_{1,2}$ and $\text{Cu}^+(\text{pyrrole})_{1,2}$ with O_2 and CO , 161

Cocaine

The effect of liquid chromatography eluents and additives on the positive ion responses of cocaine, benzoylecgonine, and ecgonine methyl ester using electrospray ionization, 247

Collision-induced dissociation

Cation- π interactions with a model for an extended π network. Absolute binding energies of alkali metal cation-naphthalene

complexes determined by threshold collision-induced dissociation and theoretical studies, 1

Sequential bond energies of $\text{Pt}^+(\text{NH}_3)_x$ ($x = 1-4$) determined by collision-induced dissociation and theory, 47

Binding of metalloporphyrins to model nitrogen bases: collision-induced dissociation and ion-molecule reaction studies, 111

Influence of substituents on cation- π interactions. 3. Absolute binding energies of alkali metal cation-aniline complexes determined by threshold collision-induced dissociation and theoretical studies, 339

Condensation reaction

Condensation reaction vs. ligand exchange with first-row transition metal cations: a theoretical study of Cu^+ heteroleptic model complexes, 587

Coulomb explosion

Comparison of methyl and hydroxyl protons generated in a Coulomb explosion event: application of a time-of-flight gating technique to methanol clusters, 577

Covalent bonds

Guided ion beam studies of transition metal-ligand thermochemistry, 289

Crown ether

Alkali metal binding energies of dibenzo-18-crown-6: experimental and computational results, 63

 Cu^+

Gas-phase kinetic measurements and quantum chemical calculations of the ligation of Ni^+ , Cu^+ , $\text{Ni}^+(\text{pyrrole})_{1,2}$ and $\text{Cu}^+(\text{pyrrole})_{1,2}$ with O_2 and CO , 161

 Cu^+ affinities

Binding energies of Cu^+ to saturated and α,β -unsaturated alkanes, silanes and germanes. The role of agostic interactions, 401

p-Cymene molecular ion

Dissociation of *p*-cymene molecular ions induced by thermal radiation, 135

Density functional theory

Stereochemical analysis of deuterated alkyl chains by charge-remote fragmentations of protonated parent ions, 175

2,5-DHB

Temperature dependence of dissociative electron attachment to molecules of gentisic acid, hydroquinone and *p*-benzoquinone, 281

1,3,2-Dioxaphospholane

Tautomerization and dissociation of ethylene phosphonate ions $[\text{OCH}_2\text{CH}_2\text{O}]\text{P}(\text{H})\text{O}^+$: an experimental and CBS-QB3 computational study, 453

Dissociation energy

Dissociation energies of silver clusters Ag_n^+ , $n = 14, 15, 16, 18$, 87

Dissociation of *p*-cymene molecular ions induced by thermal radiation, 135

Dissociative attachment

Temperature dependencies of negative ions formation by capture of low-energy electrons for some typical MALDI matrices, 259

Temperature dependence of dissociative electron attachment to molecules of gentisic acid, hydroquinone and *p*-benzoquinone, 281

- Dissociative recombination
Branching ratios for the dissociative recombination of hydrocarbon ions. I: The cases of $C_4H_9^+$ and $C_4H_5^+$, 273
- Dissociative resonance structures
Stereochemical analysis of deuterated alkyl chains by charge-remote fragmentations of protonated parent ions, 175
- Distonic ions
Proton affinity of some radicals of alcohols, ethers and amines, 373
- Dynamical studies
Comparison of methyl and hydroxyl protons generated in a Coulomb explosion event: application of a time-of-flight gating technique to methanol clusters, 577
- Dynamics
3-Dimensional structural characterization of cationized polyhedral oligomeric silsesquioxanes (POSS) with styryl and phenylethyl capping agents, 205
- Ecgonine methyl ester
The effect of liquid chromatography eluents and additives on the positive ion responses of cocaine, benzoylecgonine, and ecgonine methyl ester using electrospray ionization, 247
- Electron affinity
G3 and G2 thermochemistry of sulfur fluoride neutrals and anions, 413
- Electrospray
Structures and fragmentations of zinc(II) complexes of amino acids in the gas phase. IV. Solvent effect on the structure of electrosprayed ions, 439
- Energetic fragments
Comparison of methyl and hydroxyl protons generated in a Coulomb explosion event: application of a time-of-flight gating technique to methanol clusters, 577
- Energetics
The proton affinity scale, and effects of ion structure and solvation, 525
Proton affinities and gas-phase basicities: theoretical methods and structural effects, 601
- Energy-resolved MS
Gas-phase ion chemistry and ion thermochemistry of phenyltrifluorosilane, 303
- Enzymatic digestion
Probing the interactions of oxidized insulin chain A and metal ions using electrospray ionization mass spectrometry, 97
- ESI
An electrospray ionization-flow tube study of H/D exchange in the protonated serine dimer and protonated serine dipeptide, 77
- Femtosecond dynamics
Comparison of methyl and hydroxyl protons generated in a Coulomb explosion event: application of a time-of-flight gating technique to methanol clusters, 577
- Flow tube
An electrospray ionization-flow tube study of H/D exchange in the protonated serine dimer and protonated serine dipeptide, 77
- Flowing afterglow
New measurements of the thermochemistry of SF_5^- and SF_6^- , 361
- Fluoride affinity
G3 and G2 thermochemistry of sulfur fluoride neutrals and anions, 413
- Franck–Condon effects
The use of kinetic isotope effects for the determination of internal energy distributions in isolated transient species in the gas phase, 327
- Free electrons
Temperature dependencies of negative ions formation by capture of low-energy electrons for some typical MALDI matrices, 259
- FT-ICR
Proton affinity of some radicals of alcohols, ethers and amines, 373
- G2
G3 and G2 thermochemistry of sulfur fluoride neutrals and anions, 413
- G3
G3 and G2 thermochemistry of sulfur fluoride neutrals and anions, 413
- G2(MP2)
G3 and G2 thermochemistry of sulfur fluoride neutrals and anions, 413
- G3(MP2)
G3 and G2 thermochemistry of sulfur fluoride neutrals and anions, 413
- Gas basicity
Proton affinity of some radicals of alcohols, ethers and amines, 373
Gas phase basicity of silanaldehydes and silanones, 381
- Gas phase
Alkali metal binding energies of dibenzo-18-crown-6: experimental and computational results, 63
- Gas phase acidity
The gas and solution phase acidities of HNO, HOONO, HONO, and HONO₂, 421
Gas-phase acidities and sites of deprotonation of 2-ketones and structures of the corresponding enolates, 497
- Gas phase basicity
Application of the kinetic method to bifunctional bases. MIKE and CID-MIKE test cases, 479
- Gas-phase equilibria
Thermochemical stabilities of the gas-phase cluster ions $H_3C^+(N_2)_n$, 391
- Gas-phase ion chemistry
Gas-phase ion chemistry and ion thermochemistry of phenyltrifluorosilane, 303
- Guided ion beam
Cation- π interactions with a model for an extended π network. Absolute binding energies of alkali metal cation-naphthalene complexes determined by threshold collision-induced dissociation and theoretical studies, 1
Sequential bond energies of $Pt^+(NH_3)_x$ ($x = 1-4$) determined by collision-induced dissociation and theory, 47

- Guided ion beam studies of transition metal–ligand thermochemistry, 289
- Influence of substituents on cation– π interactions. 3. Absolute binding energies of alkali metal cation–aniline complexes determined by threshold collision-induced dissociation and theoretical studies, 339
- H/D exchange
An electrospray ionization–flow tube study of H/D exchange in the protonated serine dimer and protonated serine dipeptide, 77
- High pressure mass spectrometer
Thermochemical stabilities of the gas-phase cluster ions $\text{H}_3\text{C}^+(\text{N}_2)_n$, 391
- HPMS
Gas-phase acidities and sites of deprotonation of 2-ketones and structures of the corresponding enolates, 497
- Hybrid density functional theory
Competition between π - and σ -based interactions in metal ion complexes of the phenyl radical, 33
- Hydrogen bonds
The proton affinity scale, and effects of ion structure and solvation, 525
The structure and energetics of $[\text{B}, \text{C}, \text{F}, \text{H}_3]^+$: quantum chemistry shows multiple minima, 555
Proton affinities and gas-phase basicities: theoretical methods and structural effects, 601
- Hydrogen bridges
The structure and energetics of $[\text{B}, \text{C}, \text{F}, \text{H}_3]^+$: quantum chemistry shows multiple minima, 555
- ICP-SIFT
Gas-phase kinetic measurements and quantum chemical calculations of the ligation of Ni^+ , Cu^+ , $\text{Ni}^+(\text{pyrrole})_{1,2}$ and $\text{Cu}^+(\text{pyrrole})_{1,2}$ with O_2 and CO , 161
- Insulin chain A
Probing the interactions of oxidized insulin chain A and metal ions using electrospray ionization mass spectrometry, 97
- Internal energy distribution functions
The use of kinetic isotope effects for the determination of internal energy distributions in isolated transient species in the gas phase, 327
- Internal lysine residues
Selective cleavage at internal lysine residues in protonated vs. metalated peptides, 191
- Ion clusters
Gas-phase ion chemistry in silane/propyne mixtures, 235
- Ion solvation
The proton affinity scale, and effects of ion structure and solvation, 525
- Ion thermochemistry
Gas-phase ion chemistry and ion thermochemistry of phenyltrifluorosilane, 303
- Ion trap mass spectrometry
Gas-phase ion chemistry in silane/propyne mixtures, 235
- Ion–dipole potential
Stationary points for the $\text{OH}^- + \text{CH}_3\text{F} \rightarrow \text{CH}_3\text{OH} + \text{F}^-$ potential energy surface, 315
- Ionization energies
Thermochemistry of neutral and cationic iron hydroxides $\text{Fe}(\text{OH})_n^{0/+}$ ($n = 1, 2$) in the gas phase, 121
- Ion–ligand binding
Competition between π - and σ -based interactions in metal ion complexes of the phenyl radical, 33
- Ion–molecule reactions
Binding of metalloporphyrins to model nitrogen bases: collision-induced dissociation and ion–molecule reaction studies, 111
- Iron halides
Thermochemistry of neutral and cationic iron hydroxides $\text{Fe}(\text{OH})_n^{0/+}$ ($n = 1, 2$) in the gas phase, 121
- Iron hydroxides
Thermochemistry of neutral and cationic iron hydroxides $\text{Fe}(\text{OH})_n^{0/+}$ ($n = 1, 2$) in the gas phase, 121
- Isoelectronic species
The structure and energetics of $[\text{B}, \text{C}, \text{F}, \text{H}_3]^+$: quantum chemistry shows multiple minima, 555
- Isomeric structures
The structure and energetics of $[\text{B}, \text{C}, \text{F}, \text{H}_3]^+$: quantum chemistry shows multiple minima, 555
- Isomerization
Structures and fragmentations of zinc(II) complexes of amino acids in the gas phase. IV. Solvent effect on the structure of electrosprayed ions, 439
- Isomers
Branching ratios for the dissociative recombination of hydrocarbon ions. I: The cases of C_4H_9^+ and C_4H_5^+ , 273
- Keto–enol tautomerization
Stereochemical analysis of deuterated alkyl chains by charge-remote fragmentations of protonated parent ions, 175
- 2-Ketones
Gas-phase acidities and sites of deprotonation of 2-ketones and structures of the corresponding enolates, 497
- Kinetic isotope effects
The use of kinetic isotope effects for the determination of internal energy distributions in isolated transient species in the gas phase, 327
- Kinetic method
Gas phase basicity of silanaldehydes and silanones, 381
Application of the kinetic method to bifunctional bases. MIKE and CID-MIKE test cases, 479
The Na^+ affinities of α -amino acids: side-chain substituent effects, 509
- Kinetics
Kinetics and thermodynamics for the bonding of benzene to 20 main-group atomic cations: formation of half-sandwiches, full-sandwiches and beyond, 563
- LC
The effect of liquid chromatography eluents and additives on the positive ion responses of cocaine, benzoylecgonine, and ecgonine methyl ester using electrospray ionization, 247

- Ligand exchange
 Condensation reaction vs. ligand exchange with first-row transition metal cations: a theoretical study of Cu^+ heteroleptic model complexes, 587
- Ligation
 Gas-phase kinetic measurements and quantum chemical calculations of the ligation of Ni^+ , Cu^+ , $\text{Ni}^+(\text{pyrrole})_{1,2}$ and $\text{Cu}^+(\text{pyrrole})_{1,2}$ with O_2 and CO , 161
 Kinetics and thermodynamics for the bonding of benzene to 20 main-group atomic cations: formation of half-sandwiches, full-sandwiches and beyond, 563
- Long-lived excited state
 Anisotropic photodissociation of vinyl chloride molecular cation in the ground and first excited electronic states, 21
- Main-group atomic cations
 Kinetics and thermodynamics for the bonding of benzene to 20 main-group atomic cations: formation of half-sandwiches, full-sandwiches and beyond, 563
- Main-group metal ions
 Competition between π - and σ -based interactions in metal ion complexes of the phenyl radical, 33
- MALDI
 Temperature dependencies of negative ions formation by capture of low-energy electrons for some typical MALDI matrices, 259
 Temperature dependence of dissociative electron attachment to molecules of gentisic acid, hydroquinone and *p*-benzoquinone, 281
- Mass accuracy
 An energy-isochronous multi-pass time-of-flight mass spectrometer consisting of two coaxial electrostatic mirrors, 217
- Mass measurements
 An energy-isochronous multi-pass time-of-flight mass spectrometer consisting of two coaxial electrostatic mirrors, 217
- Mass spectrometry
 Thermochemistry of neutral and cationic iron hydroxides $\text{Fe}(\text{OH})_n^{0/+}$ ($n = 1, 2$) in the gas phase, 121
- Master equation
 Dissociation of *p*-cymene molecular ions induced by thermal radiation, 135
- Metalated complexes
 Probing the interactions of oxidized insulin chain A and metal ions using electrospray ionization mass spectrometry, 97
- Metalated peptides
 Selective cleavage at internal lysine residues in protonated vs. metalated peptides, 191
- Metal–ligand complexes
 Sequential bond energies of $\text{Pt}^+(\text{NH}_3)_x$ ($x = 1-4$) determined by collision-induced dissociation and theory, 47
- Metalloporphyrin–ligand binding
 Binding of metalloporphyrins to model nitrogen bases: collision-induced dissociation and ion–molecule reaction studies, 111
- Metalloporphyrins
 Binding of metalloporphyrins to model nitrogen bases: collision-induced dissociation and ion–molecule reaction studies, 111
- Metal–peptide interactions
 Probing the interactions of oxidized insulin chain A and metal ions using electrospray ionization mass spectrometry, 97
- MIKE spectrometry
 Anisotropic photodissociation of vinyl chloride molecular cation in the ground and first excited electronic states, 21
- Negative ions
 Temperature dependencies of negative ions formation by capture of low-energy electrons for some typical MALDI matrices, 259
 Temperature dependence of dissociative electron attachment to molecules of gentisic acid, hydroquinone and *p*-benzoquinone, 281
- Neutralization–reionization mass spectrometry
 The use of kinetic isotope effects for the determination of internal energy distributions in isolated transient species in the gas phase, 327
- Ni^+
 Gas-phase kinetic measurements and quantum chemical calculations of the ligation of Ni^+ , Cu^+ , $\text{Ni}^+(\text{pyrrole})_{1,2}$ and $\text{Cu}^+(\text{pyrrole})_{1,2}$ with O_2 and CO , 161
- Noncovalent bonds
 Guided ion beam studies of transition metal–ligand thermochemistry, 289
- O_2
 Gas-phase kinetic measurements and quantum chemical calculations of the ligation of Ni^+ , Cu^+ , $\text{Ni}^+(\text{pyrrole})_{1,2}$ and $\text{Cu}^+(\text{pyrrole})_{1,2}$ with O_2 and CO , 161
- Organoborane halide
 The structure and energetics of $[\text{B}, \text{C}, \text{F}, \text{H}_3]^+$: quantum chemistry shows multiple minima, 555
- Origin of life
 Abiotic synthesis of ATP from AMP in the gas phase: implications for the origin of biologically important molecules from small molecular clusters, 147
- 2-Oxide
 Tautomerization and dissociation of ethylene phosphonate ions $[\text{OCH}_2\text{CH}_2\text{O}]\text{P}(\text{H})\text{O}^+$: an experimental and CBS-QB3 computational study, 453
- Phenyl radical
 Competition between π - and σ -based interactions in metal ion complexes of the phenyl radical, 33
- Phenyltrifluorosilane
 Gas-phase ion chemistry and ion thermochemistry of phenyltrifluorosilane, 303
- Phosphate
 Abiotic synthesis of ATP from AMP in the gas phase: implications for the origin of biologically important molecules from small molecular clusters, 147
- Phosphonate/phosphite tautomerism
 Tautomerization and dissociation of ethylene phosphonate ions $[\text{OCH}_2\text{CH}_2\text{O}]\text{P}(\text{H})\text{O}^+$: an experimental and CBS-QB3 computational study, 453

- Photodissociation
 Anisotropic photodissociation of vinyl chloride molecular cation in the ground and first excited electronic states, 21
- Potential energy surface
 Stationary points for the $\text{OH}^- + \text{CH}_3\text{F} \rightarrow \text{CH}_3\text{OH} + \text{F}^-$ potential energy surface, 315
- Propyne
 Gas-phase ion chemistry in silane/propyne mixtures, 235
- Proteins
 Studies into the selective accumulation of multiply charged protein ions in a quadrupole ion trap mass spectrometer, 223
- Proton affinity
 Proton affinity of some radicals of alcohols, ethers and amines, 373
 Gas phase basicity of silanaldehydes and silanones, 381
 Application of the kinetic method to bifunctional bases. MIKE and CID-MIKE test cases, 479
 The proton affinity scale, and effects of ion structure and solvation, 525
 Proton affinities and gas-phase basicities: theoretical methods and structural effects, 601
- Protonated peptides
 Selective cleavage at internal lysine residues in protonated vs. metalated peptides, 191
- Protonated serine dimer
 An electrospray ionization-flow tube study of H/D exchange in the protonated serine dimer and protonated serine dipeptide, 77
- Proton-bound dimer
 Gas phase basicity of silanaldehydes and silanones, 381
- $\text{Pt}^+(\text{NH}_3)_x$
 Sequential bond energies of $\text{Pt}^+(\text{NH}_3)_x$ ($x = 1-4$) determined by collision-induced dissociation and theory, 47
- Pyrrole
 Gas-phase kinetic measurements and quantum chemical calculations of the ligation of Ni^+ , Cu^+ , $\text{Ni}^+(\text{pyrrole})_{1,2}$ and $\text{Cu}^+(\text{pyrrole})_{1,2}$ with O_2 and CO , 161
- QCISD(T)
 The structure and energetics of $[\text{B}, \text{C}, \text{F}, \text{H}_3]^+$: quantum chemistry shows multiple minima, 555
- Quadrupole ion trap mass spectrometry
 Studies into the selective accumulation of multiply charged protein ions in a quadrupole ion trap mass spectrometer, 223
- Quid-pro-quo
 Tautomerization and dissociation of ethylene phosphonate ions $[\text{OCH}_2\text{CH}_2\text{O}]\text{P}(\text{H})\text{O}^+$: an experimental and CBS-QB3 computational study, 453
- Reactivity of vinylsilanes and germanes
 Binding energies of Cu^+ to saturated and α,β -unsaturated alkanes, silanes and germanes. The role of agostic interactions, 401
- Reflectron
 3-Dimensional structural characterization of cationized polyhedral oligomeric silsesquioxanes (POSS) with styryl and phenylethyl capping agents, 205
- RRKM calculations
 The use of kinetic isotope effects for the determination of internal energy distributions in isolated transient species in the gas phase, 327
- Salt bridge
 Abiotic synthesis of ATP from AMP in the gas phase: implications for the origin of biologically important molecules from small molecular clusters, 147
 The Na^+ affinities of α -amino acids: side-chain substituent effects, 509
- Selective accumulation
 Studies into the selective accumulation of multiply charged protein ions in a quadrupole ion trap mass spectrometer, 223
- Selective cleavage C-terminal to lysine
 Selective cleavage at internal lysine residues in protonated vs. metalated peptides, 191
- Sequential bond energies
 Sequential bond energies of $\text{Pt}^+(\text{NH}_3)_x$ ($x = 1-4$) determined by collision-induced dissociation and theory, 47
- SF_5^-
 New measurements of the thermochemistry of SF_5^- and SF_6^- , 361
- SF_6^-
 New measurements of the thermochemistry of SF_5^- and SF_6^- , 361
- SF
 G3 and G2 thermochemistry of sulfur fluoride neutrals and anions, 413
- SF_2
 G3 and G2 thermochemistry of sulfur fluoride neutrals and anions, 413
- SF_2^-
 G3 and G2 thermochemistry of sulfur fluoride neutrals and anions, 413
- SF_3
 G3 and G2 thermochemistry of sulfur fluoride neutrals and anions, 413
- SF_3^-
 G3 and G2 thermochemistry of sulfur fluoride neutrals and anions, 413
- SF_4
 G3 and G2 thermochemistry of sulfur fluoride neutrals and anions, 413
- SF_4^-
 G3 and G2 thermochemistry of sulfur fluoride neutrals and anions, 413
- SF_5
 G3 and G2 thermochemistry of sulfur fluoride neutrals and anions, 413
- SF_5^-
 G3 and G2 thermochemistry of sulfur fluoride neutrals and anions, 413
- SF_6
 G3 and G2 thermochemistry of sulfur fluoride neutrals and anions, 413

- SF₆⁻
G3 and G2 thermochemistry of sulfur fluoride neutrals and anions, 413
- SF⁻
G3 and G2 thermochemistry of sulfur fluoride neutrals and anions, 413
- Silanaldehydes
Gas phase basicity of silanaldehydes and silanones, 381
- Silane
Gas-phase ion chemistry in silane/propyne mixtures, 235
- Silanones
Gas phase basicity of silanaldehydes and silanones, 381
- Silver clusters
Dissociation energies of silver clusters Ag_n⁺, *n* = 14, 15, 16, 18, 87
- S_N2 reactions
Stationary points for the OH⁻ + CH₃F → CH₃OH + F⁻ potential energy surface, 315
- Sodium ion affinities
The Na⁺ affinities of α-amino acids: side-chain substituent effects, 509
- Solvation effects
The gas and solution phase acidities of HNO, HOONO, HONO, and HONO₂, 421
- Solvent effects
Structures and fragmentations of zinc(II) complexes of amino acids in the gas phase. IV. Solvent effect on the structure of electrosprayed ions, 439
- Structural effects
Proton affinities and gas-phase basicities: theoretical methods and structural effects, 601
- Substituent effects
Proton affinities and gas-phase basicities: theoretical methods and structural effects, 601
- SWIFT
Studies into the selective accumulation of multiply charged protein ions in a quadrupole ion trap mass spectrometer, 223
- Tandem mass spectrometry
Probing the interactions of oxidized insulin chain A and metal ions using electrospray ionization mass spectrometry, 97
Tautomerization and dissociation of ethylene phosphonate ions [OCH₂CH₂O]P(H)O⁺: an experimental and CBS-QB3 computational study, 453
How does chlorine substitution on acetonitrile affect the internal S_N2 isomerization of proton-bound pairs (ClCH₂CN)(ROH)H⁺ (R = CH₃, C₂H₅, C₃H₇)?, 471
- Thermochemistry
Guided ion beam studies of transition metal–ligand thermochemistry, 289
New measurements of the thermochemistry of SF₅⁻ and SF₆⁻, 361
The proton affinity scale, and effects of ion structure and solvation, 525
Proton affinities and gas-phase basicities: theoretical methods and structural effects, 601
- Thermodynamics
Kinetics and thermodynamics for the bonding of benzene to 20 main-group atomic cations: formation of half-sandwiches, full-sandwiches and beyond, 563
- Time-of-flight mass spectrometer
An energy-isochronous multi-pass time-of-flight mass spectrometer consisting of two coaxial electrostatic mirrors, 217
- Transition metal
Condensation reaction vs. ligand exchange with first-row transition metal cations: a theoretical study of Cu⁺ heteroleptic model complexes, 587
- Transition metal ions
Guided ion beam studies of transition metal–ligand thermochemistry, 289
- Unimolecular reactions
How does chlorine substitution on acetonitrile affect the internal S_N2 isomerization of proton-bound pairs (ClCH₂CN)(ROH)H⁺ (R = CH₃, C₂H₅, C₃H₇)?, 471
- Vicinal elimination
Stereochemical analysis of deuterated alkyl chains by charge-remote fragmentations of protonated parent ions, 175
- Vinyl chloride ion
Anisotropic photodissociation of vinyl chloride molecular cation in the ground and first excited electronic states, 21
- VUV photoionisation
Proton affinity of some radicals of alcohols, ethers and amines, 373
- Zinc
Structures and fragmentations of zinc(II) complexes of amino acids in the gas phase. IV. Solvent effect on the structure of electrosprayed ions, 439
- Zwitterion
Stereochemical analysis of deuterated alkyl chains by charge-remote fragmentations of protonated parent ions, 175